Structure and Properties of Liquid Methanol[1]

William L. Jorgensen[2]

Contribution from the Department of Chemistry, Purdue University, West Lafayette, Indiana 47907. *Received July 2, 1979*

Abstract: Statistical mechanics simulations of liquid methanol at 25 °C have been carried out using an intermolecular potential function derived from ab initio molecular orbital calculations with added dispersion corrections. Detailed structural and thermodynamic information has been obtained and compares favorably with the available experimental results including X-ray and infrared data. The liquid primarily consists of long, winding hydrogen bonded chains. Roughly linear hydrogen bonding dominates. Most monomers (56%) are in two hydrogen bonds; 24 and 17% are in one and three hydrogen bonds, respectively, and there is 2.5% monomer present in the liquid. Stereoplots give little indication of dimers, though various higher oligomers are evident. The singly hydrogen bonded monomers occur at the ends of chains, while the monomers with three hydrogen bonds are at Y junctions. For the first time in a liquid simulation, the binding energy distribution is found to be bimodal rather than unimodal. The higher energy peak is proved to be due to the singly hydrogen bonded monomers. Overall, the results confirm the capabilities of computer-simulation techniques to successfully model complex fluids.

I. Introduction

Alcohols appear to have first been isolated by distillation in the 12th century. The medicinal value of ethanol was certainly known to the 13th century Latin physicians, Thaddeus Alderotti and Arnold of Villanova. Perhaps it is not surprising that it is more difficult to identify the early discoverers of methanol. However, by 1661 Robert Boyle had separated wood distillates into two fractions, a component of which was recognized by Dumas and Péligot in 1834 as the simplest alcohol. Berthelot in 1857 performed the first synthesis of methanol from methyl chloride.[4] Methanol is now made by catalytic hydrogenation of carbon monoxide to the extent of over one billion gallons per year in the U.S. alone. Besides its use as a solvent, methanol is the key precursor of formaldehyde and its potential as a fuel is receiving increased attention.[5]

Methanol is also fascinating since like water its condensed-phase properties are strongly influenced by hydrogen bonding. A detailed knowledge of hydrogen bonding has important applications in many areas including liquid theories, solvent effects in organic chemistry, and the structure and reactivity of biomolecules. In recent publications, we have reported statistical mechanics simulations of liquid water[6] and hydrogen fluoride.[7] In-depth analyses of the liquids' structures and hydrogen bonding have been included. The necessary intermolecular potential functions were derived from ab initio molecular orbital computations. Furthermore, the dependence of the results on the sophistication of the ab initio calculations has been examined.[3,6,7] As described here, the studies have now been extended to include liquid methanol. This is a significant addition due to the increase in size for the system, the presence of nonpolar groups, and since this is the first computer simulation of an alcohol.

The studies of water showed that the quality of the results for the liquid is not enhanced smoothly as the ab initio calculations become more sophisticated.[6] In fact, potential functions representative of minimal basis set and large basis set plus configuration interaction (CI) calculations were found to yield similar structural and thermodynamic results for liquid water. Intermediate levels of theory are generally less successful owing primarily to their poorer estimates of the dimerization energies of second-row hydrides. Consequently, an intermolecular potential function for the methanol dimer was obtained from minimal basis set calculations.[3] However, it was necessary to correct the methyl–methyl and O–H dispersion terms in accordance with accurate models for the methane and water dimers.[3] Such adjustment is logical since ab initio calculations within the Hartree–Fock limit do not explicitly consider dispersion effects. Also, the magnitude of dispersion interactions increases along the series HF, H_2O, NH_3, CH_4 roughly in proportion to the polarizability squared.[8] Thus, it is critical to have the short-range interactions between alkyl groups properly represented in potential functions.

As discussed here, the modified potential yields structural and energetic results for liquid methanol in good agreement with experimental data, particularly when the neglect of three-body interactions is taken into account. In addition, the computer simulations permit a thorough analysis of the structure of the liquid through energetic and hydrogen-bonding distributions as well as from stereoviews of configurations of the modeled system. Liquid methanol is found to consist primarily of long, winding hydrogen-bonded chains with roughly linear hydrogen bonds. Monomers are in from one to three hydrogen bonds corresponding to free monomers and monomers at the ends, in the interior, and at Y junctions of chains. Another highlight is the first occurrence of a bimodal binding energy distribution and its decomposition. This study also further establishes the potential for computer modeling of complex fluids containing both hydrogen bonding and nonpolar interactions as found in biochemical systems.[9] However, it should again be emphasized that extensions involving much stronger forces such as in ionic solutions must be approached cautiously in view of the potential importance of three-body and higher order effects.

II. Computational Details

A. Potential Functions. The key components in Monte Carlo or molecular dynamics simulations for a liquid are intermolecular potential functions for the constituent dimers. These functions are obtained either empirically or from ab initio molecular orbital calculations. A serious drawback to the empirical approach is the shortage of accurate gas-phase data for dimers. The obvious advantage to the quantum-mechanical route is that potential functions can be derived for systems that have received little or no experimental examination. A complication is that the potentials depend on the choices of basis set and correlation energy corrections in the ab initio calculations.

Following earlier work,[6,7b] an intermolecular potential function for the methanol dimer was generated from ab initio calculations with the minimal STO-3G basis set.[3] Dimerization energies for 270 points on the potential surface, selected by the iterative energy distributed random geometries procedure, were fit to a 12-6-1 potential function. The monomers were held rigid in the staggered conformation and the geometric parameters were taken from a microwave determination.[10] Specifically, the OH, CH, and CO bond lengths are 0.9451,

0002-7863/80/1502-0543$01.00/0

Table I. Parameters in the 12-6-1 Potential Functions for $(CH_3OH)_2$[a]

12-6-1 Potential		
q_L[b]	q_H	q_{Me}
−2.716 198	3.424 811	(2.007 585)[c]
	R_{OL} = 0.754 726 0	
	c	d
OO	−457.0440	504358.3
HH	95.70276	621.4455
MeMe	3097.009	670395.2
OH	−201.9707	1286.560
OMe	−966.8230	772968.9
HMe	290.1323	35961.24
D-12-6-1 Potential		
c(MeMe) = 247.009		c'(OH) = −155.
r_m = 2.7		r_0 = 1.7

[a] All values correspond to energies in kcal/mol and distances in ångstroms. [b] Two-point charges (L) are placed on the COH bisector at distances of R_{OL} from the oxygen and with ∠LOL = 109.47°. [c] Value determined from neutrality.

1.0936, and 1.4246 Å and the COH and HCO angles are 108.533 and 110.297°.

For the potential function, a five-center model was used to represent a monomer. The sites are the oxygen atom, hydroxyl hydrogen, two pseudo-lone pairs placed tetrahedrally on the oxygen, and the methyl group, which was treated as a unit centered on the carbon. The function is given in eq 1 and the adjustable parameters are listed in Table I.

$$\Delta E(12\text{-}6\text{-}1) = \sum_{i<j}^{\text{charges}} \frac{q_i q_j}{r_{ij}} + \sum_{\mu<\nu}^{\text{atoms}} \left(\frac{c_{mn}}{r_{\mu\nu}^{6}} + \frac{d_{mn}}{r_{\mu\nu}^{12}} \right) \quad (1)$$

As usual, physical significance should not be attributed to individual parameter values.[3] For the Coulombic term, charges were placed on the lone pairs, the hydrogen and carbon. The second sum which represents the short-range interactions is over pairs of atoms (H, O, methyl (Me)) with types m and n in the different monomers. The standard deviation of the fit of the potential to the dimerization energies for bound pairs ($\Delta E < 0$) was excellent (0.36 kcal/mol).[3] Including repulsive points with ΔE up to +5 kcal/mol raises the standard deviation to 0.51 kcal/mol. In view of the simple representation of the methyl group, the overall fit is certainly acceptable. The predictions for the geometries and dimerization energies for the linear and cyclic dimers from the 12-6-1 potential are also in good agreement with optimized STO-3G values. For the linear dimer, the 12-6-1 potential yields for R_{OO}, θ, and ΔE 2.644 Å, 41.8°, and −6.33 kcal/mol. The dimerization energy after

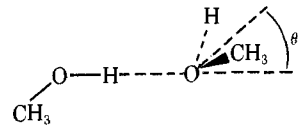

adjustment to an enthalpy change falls near the end of the experimental range (−3.2 to −4.5 kcal/mol).[11] The cyclic dimer is predicted to be less stable (ΔE = −2.38 kcal/mol) as for water and hydrogen fluoride.[6,7]

Analysis of accurate potential functions for methane dimers revealed that STO-3G calculations underestimate the attraction of nonpolar groups.[3] Also, comparison of the well shapes for the linear water dimers from STO-3G and CI calculations showed that the STO-3G well is too narrow.[6] This causes the first peak in the OO radial distribution function for liquid water to be too sharp with the STO-3G potential. Therefore, modifications were made to the 12-6-1 potential to help correct these deficiencies. The MeMe dispersion coefficient (c_{MeMe}) was reduced by 2850 and a scaled dispersion term was added to the O···H interactions. Its form is $C'_{OH} r_{OH}^{-6} f(r)$ where $f(r)$ is the scaling function of Rahman and Stillinger:[12]

$$f(r) = (r - r_0)^2 (3r_m - r_0 - 2r)(r_m - r_0)^{-3} \quad (2)$$

The modified potential was designated D-12-6-1. The additional parameters are recorded in Table I. Besides broadening the hydrogen-bonding well, the dimerization energies for the linear and cyclic dimers are lowered to −6.91 and −3.80 kcal/mol by the D-12-6-1 potential. The geometric predictions are essentially unchanged. Full details on the potential functions are presented elsewhere.[3]

B. Monte Carlo Simulations. Monte Carlo statistical mechanics simulations were executed for liquid methanol using the 12-6-1 and D-12-6-1 potentials. Cubic samples of 128 methanol molecules (640 particles) were treated with periodic boundary conditions. The simulations were run with a temperature of 25 °C and at the experimental density, 0.786 64 g/cm^3.[13] Thus, the length of an edge of the periodic cube was 20.534 Å. The calculations were carried out in the standard manner using the Metropolis sampling algorithm. The details of Monte Carlo simulations may be found in simplified[7a] and sophisticated[14] forms in the literature. The energy of a configuration was obtained from the pairwise addition of the dimerization energies, as usual:

$$E_i = \sum_{a<b} \Delta E_{ab} \quad (3)$$

The neglect of higher order terms in the series is of special concern for hydrogen-bonded multimers. In particular, several investigators have calculated constructive three-body effects for head-to-tail methanol and water trimers amounting to ca. 1 kcal/mol per hydrogen bond or roughly 15% of the interaction energy.[15-17] The influence of three-body effects on the present results is considered below.

A spherical cutoff for the potentials was used at an OO separation of 8 Å. Increasing the cutoff radius to 10 Å yielded negligible change to the computed energy. As usual in Monte Carlo simulations, but not in molecular dynamics, corrections were not made for interactions with molecules beyond the cutoff. Owicki and Scheraga have estimated this effect on the energy of water in their Monte Carlo work to be only −0.15 kcal/mol for a sample of 64 molecules.[18] This is not significant in view of the fit and nature of the potential functions, the statistical fluctuations in Monte Carlo calculations, and the neglect of multibody interactions. The larger sample size in this study should also reduce the effect.

Each move to create a new configuration involved picking a molecule at random, translating it in all three Cartesian directions, and rotating it about one randomly chosen axis. The ranges for the translations and rotations were ±0.16 Å and ±15°, which provided an acceptance rate of ca. 50% for new configurations. The simulations were initiated with the monomers in an arrangement reminiscent of solid methanol.[19] Each run involved roughly 900 000 attempted moves. Control functions[14] demonstrated that the ensembles reached equilibrium within 300 000 attempted moves; however, the final averaging for properties and distribution functions was performed over only the last 400 000 configurations. The initial 500 000 configurations were discarded. Although there has been some concern about convergence in Monte Carlo simulations,[20,21] convergence has not been a noticeable problem in our investigations. For example, the average energy over each increment of 5000 attempted moves, after the initial 300 000 attempted moves, oscillated *uniformly* within a 0.25 kcal/mol range in the runs for methanol. This range corresponds to roughly 5% of the total energy. The pattern agrees with Bev-

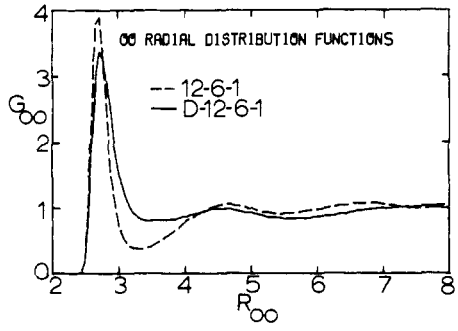

Figure 1. OO radial distribution functions for liquid methanol at 25 °C computed with the 12-6-1 and D-12-6-1 potential functions.

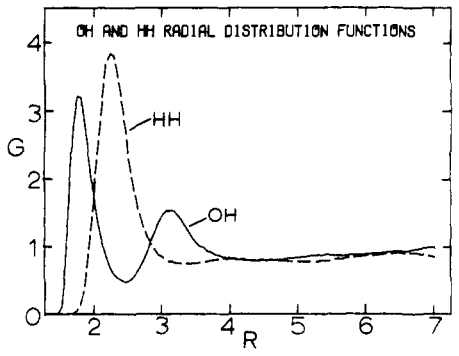

Figure 2. OH and HH radial distribution functions for liquid methanol computed with the D-12-6-1 potential function.

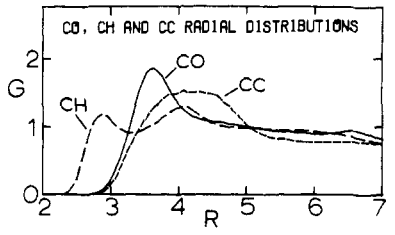

Figure 3. CO, CH, and CC radial distribution functions for liquid methanol computed with the D-12-6-1 potential function.

eridge's observations with the CI potential for water.[21] By analogy, the potential errors in our runs of ca. 10^6 configurations are ca. 1% for the energy and 3% for the radial distribution functions.[21] The only property typically computed in Monte Carlo simulations that requires substantially longer runs to guarantee convergence is the heat capacity. Errors of roughly 20% may be anticipated in this case.[21]

The Monte Carlo computations were carried out on the CDC/7600 system at the Lawrence Berkeley Laboratory. The CDC/6500-6600 system at Purdue was used for analyses and plotting.

III. Results and Discussion

A. Radial Distribution Functions. Radial distribution functions, $g_{xy}(r)$, describe the probability of occurrence of atoms with type y about atoms with type x as a function of xy separation, r, in the liquid. The relationship is

$$g_{xy}(R) = \frac{\langle N_y(R, R + \mathrm{d}R)\rangle}{\rho_y 4\pi R^2 \,\mathrm{d}R} \tag{4}$$

The numerator is the average number of y atoms in the shell between R and $R + \mathrm{d}R$, while the denominator normalizes the distribution so $g_{xy} = 1$ when N_y is the same as expected from the bulk density of y atoms, ρ_y. Peaks in $g(r)$ can often be assigned to features of the local intermolecular structure in liquids. Experimentally, radial distribution functions are determined from X-ray and neutron diffraction. Methanol has been examined with X-rays by Harvey and Wertz and Kruh.[22] Although the work is not as refined as Narten's studies of water,[24] some peak positions and areas have been obtained.

The results for g_{OO} from the 12-6-1 and D-12-6-1 potentials are compared in Figure 1. As intended, the first peak is lowered and broadened by the dispersion corrections. In both cases the maximum occurs at 2.70 Å, in agreement with the X-ray results.[22,23] The accord is fortuitous in that the potential functions probably underestimate the true OO distance in the gas-phase dimer by 0.1–0.2 Å.[3] Lipscomb's data for the solid at −110 °C and at a density of 0.98 g/cm^3 give the OO separation as 2.66 Å with the monomers arranged in parallel, hydrogen-bonded chains (Scheme I).[19]

Coordination numbers may be obtained by integrating the radial distribution functions. From the first peak in the X-ray results for the liquid,[22] each oxygen has two nearest neighbors

Scheme I

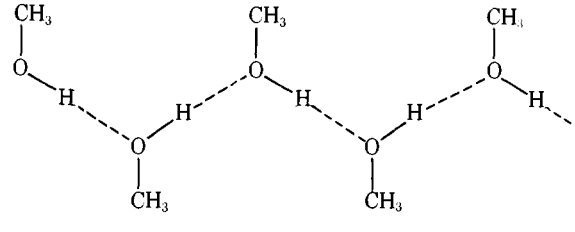

which is consistent with the local structure for the solid. Integration up to the first minimum of g_{OO} from the 12-6-1 (3.31 Å) and the D-12-6-1 potentials (3.47 Å) yields 1.9 and 2.6 neighbors, respectively. The choice of integration limit is somewhat arbitrary as is the deconvolution of the X-ray data, so the theoretical and experimental results are basically in agreement. The occurrence of the weak second maximum at 4.68 (12-6-1) and 4.55 Å (D-12-6-1) is also consistent with Lipscomb's picture and implies an average OOO angle of 115–120°. The angle in the solid is 122°.[19]

The OH, HH, CO, CH, and CC radial distribution functions from the D-12-6-1 potential are shown in Figures 2 and 3. The results from the 12-6-1 potential are generally similar except that the peaks are thinner and as much as 25% higher. This is an undesirable consequence of the narrower hydrogen-bonding wells from the 12-6-1 potential. As discussed below, the computed energy for the liquid is also too high with the 12-6-1 potential. Therefore, the following presentations will focus on the results from the D-12-6-1 function.

The two peaks in g_{OH} occur at 1.77 and 3.09 Å. Integration to the first minimum (2.48 Å) yields 1.01 hydrogens which can be assigned to the hydrogen in the adjacent hydrogen bond donating monomer. At this time, it should be pointed out that the detailed hydrogen-bonding analysis below establishes that the pattern in Scheme I, though useful as a rough guide, is an oversimplification for the liquid. Actually, the monomers do have an average of two hydrogen bonds each; however, only 56% are in exactly two hydrogen bonds.

The second peak in g_{OH} contains roughly two additional hydrogens which can also be readily assigned from Scheme I. The first peak in g_{HH} has its maximum at 2.26 Å and minimum at 3.42 Å. Integration to the minimum clearly overestimates the area in this case. Integration to the point where $g_{HH} = 1$ (2.89 Å) yields 2.4 hydrogens, whereas integration to the minimum reveals 3.3 hydrogens. Two hydrogens would be expected from Scheme I. Since liquid methanol has not yet been examined by neutron diffraction, no experimental data are available on the radial distribution functions involving hydrogen.

The distribution functions involving the methyl group in

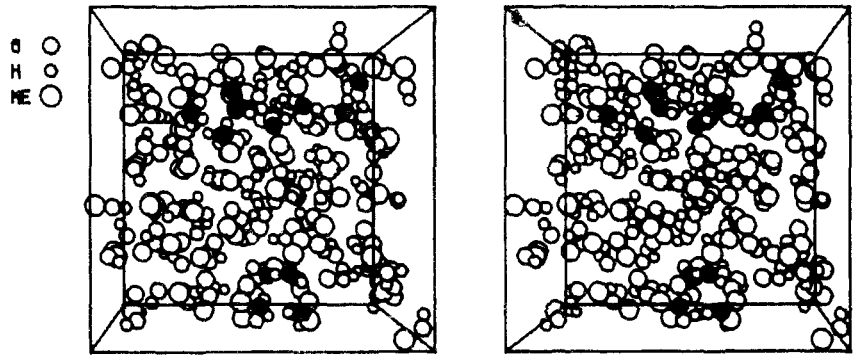

Figure 4. Stereoplot of a configuration from the simulation of liquid methanol with the D-12-6-1 potential function. The darkened oxygens near the top of the figure point out a long hydrogen bonded chain, while those near the bottom appear to be in a cyclic tetramer. The periodic cube contains 128 monomers.

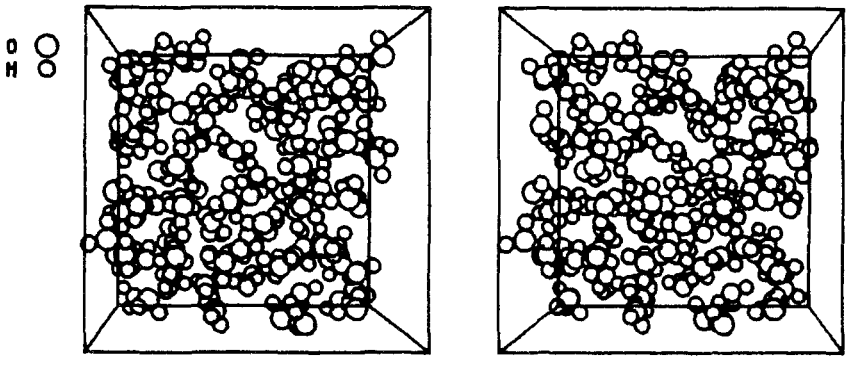

Figure 5. Stereoplot of a configuration from the simulation of liquid water at 25 °C with the STO-3G potential function (ref 6). Monomers in three and four hydrogen bonds dominate. The periodic cube contains 125 molecules.

Figure 3 are less structured. The maximum in the CO distribution occurs at 3.64 Å in reasonable accord with the X-ray peak at 3.8 Å.[22] Integration to 4.2 Å yields four oxygens which includes both intra- and interchain nearest neighbors. The CH distribution has maxima at 2.87 and 4.08 Å. The former peak integrates to about one hydrogen which is from the hydrogen-bond donor, and the second peak contains three to four additional hydrogens which again includes contacts beyond the parent chain. The CC distribution shows a broad band from 3 to 5 Å which could be decomposed into two peaks, the near peak due to interchain neighbors and the far peak due to intrachain neighbors at about the same separation as the second peak in g_{OO} (4.55 Å). Experimentally, CC bands have been assigned at 3.8 and 4.4 Å.[22] Overall, the peak positions and integrations from the X-ray data and the D-12-6-1 results are in good agreement. On this basis and from earlier studies of water[6,25] and liquid argon,[26] it is anticipated that three-body interactions have minor influence on the radial distribution functions. Previous experience also suggests that some of the peak heights may be exaggerated by as much as 25–30% in the D-12-6-1 results.[3,6,25]

B. Stereoplots and Density. The most direct way to assess the liquid's structure is to display configurations of the periodic cube. The stereoplot in Figure 4 shows a typical configuration from the D-12-6-1 simulation. Owing to the periodicity, it must be remembered that monomers near one face of the cube can be hydrogen bonded to monomers on the opposite face.

Several features are immediately apparent from the figure. (1) The monomers are evenly distributed in the cube, so the pressure is either reasonable or too high (vide infra). (2) Hydrogen bonding is ubiquitous. (3) Most monomers occur in hydrogen-bonded chains with length three or more. The chains are highly bent and winding. The blackened oxygens near the top of the figure illustrate a chain of at least eight monomers. (4) Lower oligomers are also present including what appears to be a cyclic tetramer that has been blackened near the bottom of the figure. There is much evidence for the special stability of cyclic methanol tetramers in the gas phase.[11,16] (5) There is little indication of dimers. (6) Most monomers are in two hydrogen bonds. The monomers at the ends of chains have one hydrogen bond, while monomers with three hydrogen bonds are also apparent. The latter occur at Y junctions of chains. These observations are quantified below. (7) Compared to the solid,[19] liquid methanol is highly disordered; however, the local hydrogen bonding and chain structure persist.

Since it has not been published previously, a stereoplot from our simulation of liquid water with the STO-3G potential is displayed in Figure 5.[6] The structure of water is dramatically different from methanol since each monomer is in three to four hydrogen bonds. The chains in methanol are replaced by distorted, interconnected rings in liquid water. However, the channels in ice I are at most a faint memory.

Pressure is not normally computed in Monte Carlo simulations owing to the extra computation needed in calculating the forces. Also, pressure is known to be sensitive to the inclusion of three-body interactions.[26] Nevertheless, to obtain some indication of possible errors in the computed density, the "total density fluctuation" defined by eq 5 was introduced.[7b]

$$\Delta\rho(R) = 1 + \int_0^R 4\pi\rho r^2 g(r)\mathrm{d}r - 4/3\pi R^3\rho \qquad (5)$$

The function gives the difference in the number of neighbors calculated from a radial distribution function and that expected assuming uniform density in the periodic cube. As R gets large, $\Delta\rho$ must approach zero, so the function is most informative at short range. The results using g_{OO} from the D-12-6-1 potential are shown in Figure 6. The density fluctuations are very modest

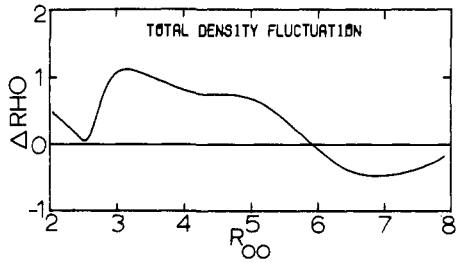

Figure 6. The total density fluctuation computed from the OO radial distribution function as defined in eq 5.

Table II. Thermodynamic Properties for Liquid Methanol at 25 °C[a]

	calcd		
	12-6-1	D-12-6-1	exptl[b]
$-E_i$	2.81	6.09	(8.48)[c]
$-E$	0.74	4.02	(6.41)[c]
$\Delta H_{vap}°$	3.40	6.68	9.07
C_v	14.2	16.7	15.9[d]

[a] Energies in kcal/mol; C_v in cal/mol·K. E_i is the internal potential energy. E and C_v include the classical kinetic energy contributions. [b] See text and ref 13. [c] Estimated. [d] Calculated from experimental coefficients of expansivity and compressibility, and C_p (ref 13).

in comparison to the simulations of liquid hydrogen fluoride which had excesses of two to six neighbors at 7.5 Å.[7b] The deviations are even smaller for the 12-6-1 potential. Thus, on this basis, it appears that the pressure in the present simulations is near normal.

C. Thermodynamics. Calculated and experimental values for the internal energy, energy, heat of vaporization to the ideal gas, and heat capacity at 25 °C are assembled in Table II. The energy and heat capacity include corrections of $^7/_2RT$ and $^7/_2R$ for the classical kinetic energy of rotation and translation of the monomers. The experimental enthalpy of vaporization has been adjusted for the nonideality of the gas.[13] The calculated enthalpy of vaporization is obtained from the internal energy and liquid density:

$$\Delta H_v° \approx -E_i(l) + P(V°(g) - V(l))$$

The experimental C_p is 19.4 cal/mol·K.[13] In general, C_v is lower than C_p; however, they are nearly identical for water at 25 °C. Standard deviations (2σ) for the computed values were obtained from control functions[14] and are less than 0.05 kcal/mol and 5 cal/mol·K for the energies and heat capacities.

The energy from the 12-6-1 potential is much too high. This can be attributed to the overestimate of the repulsion between methyl groups and the narrowness of the hydrogen-bonding wells.[3] The higher energy is accompanied by a lower heat capacity. It is notable that the radial distribution functions from the 12-6-1 potential are not absurd.

The D-12-6-1 potential yields significant improvement in the energy, although it is still overestimated by 2.4 kcal/mol. The neglect of three-body effects certainly accounts for 1-2 kcal/mol of the difference.[15-17] Any remainder may be attributed to various sources including the simple representation of the monomers in the potential function, the lack of internal rotation and vibrations, and inadequacies in the STO-3G potential surface even after the dispersion corrections. The computed heat capacity continues the pattern of good estimates as found for water and hydrogen fluoride.[6,7] The ideal gas C_p for methanol at 25 °C is 10.5 cal/mol·K, which implies that the classical treatment for C_v probably leads to a 1-2 cal/mol·K underestimate. Three-body effects should also raise the liquid's C_v somewhat; however, any discussion of computed heat capacities must keep in mind their slow convergence in Monte Carlo calculations.[20,21]

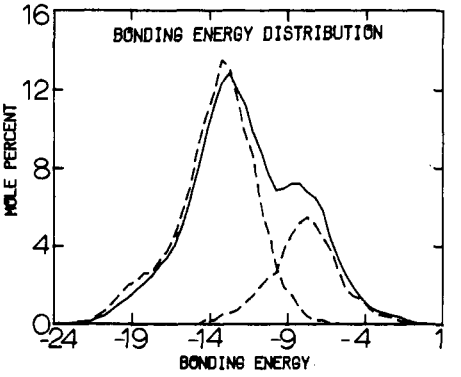

Figure 7. The distribution of binding energies for monomers in liquid methanol. The dashed lines show the separate distributions for monomers in zero or one hydrogen bond (at higher energy) and for those in multiple hydrogen bonds. The units for the y axis are mol %/kcal mol^{-1}.

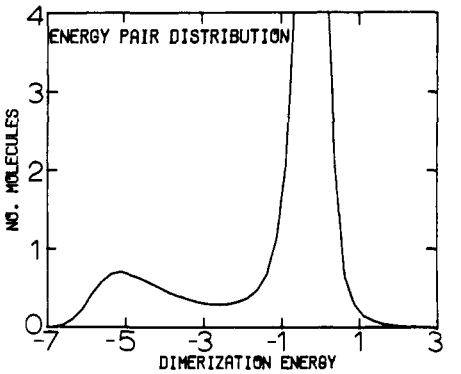

Figure 8. Distribution of dimerization energies for a monomer in liquid methanol. Dimerization energies are in kcal/mol. The units for the y axis are molecules/kcal mol^{-1}

D. Energy Distribution Functions. The distribution of binding energies for the monomers in the liquid from the D-12-6-1 potential is shown in Figure 7. The methanol monomers experience a continuum of energetic environments covering more than a 20 kcal/mol range. For the first time in a liquid simulation, the distribution is clearly bimodal rather than unimodal.[6,7,25b] As discussed below, the peak at higher energy is due to the singly hydrogen bonded monomers.

The energy pair distribution is shown in Figure 8. The ordinate gives the average number of molecules that are bound to a monomer with the dimerization energy shown on the abscissa. The minimum in the D-12-6-1 potential restricts the minimum energy to −6.9 kcal/mol. Most interactions involve distant molecules and have energies between ±1 kcal/mol. As for water and hydrogen fluoride,[6,7] the peak at low energy results from the hydrogen-bonded neighbors. The minimum occurs at −2.5 kcal/mol, which may be interpreted as the upper limit for a hydrogen-bond energy. A nearly identical value was obtained for hydrogen fluoride (−2.4 kcal/mol)[7] and the minimum for water is at −2.1 kcal/mol.[6] Integration up to the minimum indicates that each methanol monomer takes part in an average of 1.9 hydrogen bonds in agreement with the rough estimates of two from the radial distribution functions and stereoplots.

The energy distributions from the 12-6-1 potential are similar in shape to Figures 7 and 8, but shifted to higher energy. The binding energy distribution is again clearly bimodal.

E. Hydrogen Bond Distributions and Infrared Data. Con-

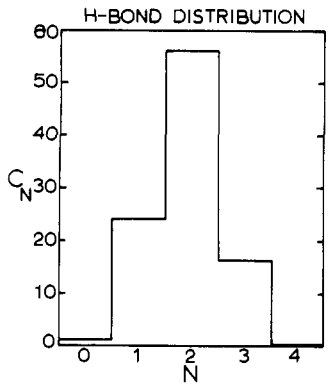

Figure 9. Distribution of coordination numbers for hydrogen-bonded neighbors from the simulation with the D-12-6-1 potential function. The units for the y axis are mol %. A hydrogen bond is defined by a dimerization energy below −2.5 kcal/mol.

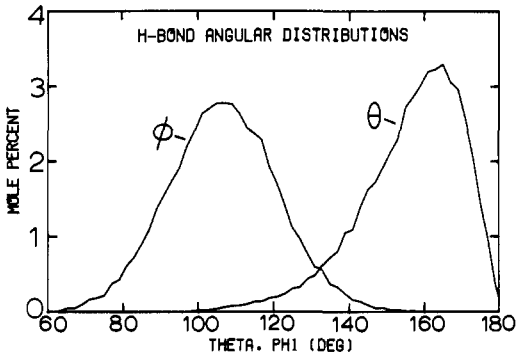

Figure 10. Distributions for the hydrogen-bonding angles between monomers with dimerization energies below −2.5 kcal/mol. The units for the y axis are mol %/deg. θ is the O-H···O angle and ϕ is the H···O-H angle.

figurations were stored every 2000 attempted moves during the Monte Carlo runs. After the hydrogen-bonding limit has been established from the energy pair distribution, the saved configurations can be analyzed to obtain a detailed description of the hydrogen bonding.[7b]

The distribution of coordination numbers is shown in Figure 9. The percentages of monomers in zero to four hydrogen bonds are 2.5, 24.2, 56.1, 16.5, and 0.6%, respectively, again giving an average of 1.9 hydrogen bonds per monomer. From the preceding discussions, the monomers with one to three hydrogen bonds are assigned to species at the ends of chains, in the middle of chains or in rings, and at Y junctions of chains.

A wealth of fascinating information has been obtained on hydrogen-bonded liquids from infrared measurements.[27] Luck has studied the concentration dependence of the O-H overtone spectra of methanol and ethanol in CCl_4 and has concluded that the pure liquids contain about 2% free monomer at room temperature.[28] The agreement with the computed value of 2.5% is good. Sandorfy has also made an important overtone study on pure methanol and provides clear evidence for polymers, oligomers, and monomers in the liquid at 25 °C.[29] The nature of the oligomers has not been clarified by the IR work. On the basis of the stereoplots, trimers and tetramers are predicted to be the dominant oligomers. In view of the present analysis, an alternative interpretation of the four bands in the overtone region worth considering is that they are due to monomers in zero, one, two, and three hydrogen bonds corresponding to free monomer, chain ends, polymer, and Y junctions.

At this point, the origin of the two bands in the binding energy distribution can be easily rationalized. It was noticed that the higher energy peak contains roughly 25% of the monomers, which is about the same as the number of monomers in zero and one hydrogen bonds. Therefore, separate binding energy distributions were generated for the monomers in zero and one hydrogen bonds and the multiply bonded monomers. The results are shown by the dashed curves in Figure 7 and confirm the hypothesis. It should be noted that the resolution for the dashed curves is less than for the solid curve, since the averaging for the former was only over the final 100 saved configurations instead of all 400 000. Clearly, the free monomers and chain ends are energetically distinct from the bulk. It is likely that the inclusion of three-body interactions would increase the fraction of polymer and reduce the amounts of monomer and singly hydrogen bonded species; however, the latter should remain energetically distinct and be detectable. For hydrogen fluoride, 18% of the monomers were found in no or one hydrogen bond; however, the energy distribution appears unimodal.[7b]

Finally, the distributions for the hydrogen-bonding angles, θ (O-H···O) and ϕ (H···O-H), are given in Figure 10. The peaks for θ and ϕ are at 166 and 107°. From the θ distribution, the average hydrogen bond is bent by ca. 15°, so linearity does not seem to dominate. However, it has been pointed out previously that it is more appropriate to plot the percentage of hydrogen bonds per unit solid angle as a function of θ, i.e., by dividing the distribution by sin θ.[30] When applied to the θ distribution in Figure 10, the preference for linear hydrogen bonding is reaffirmed. Distributions for θ have been obtained from neutron diffraction experiments on numerous solids involving a variety of X-H···Y hydrogen bonds.[30] The results with a maximum at 170° and a range to 105° are very similar to the present distribution for θ.[30] The distribution for ϕ is centered at the value expected from the optimum geometry for the linear methanol dimer. An additional item implied by Figure 10 is that cyclic dimers must be insignificant in the liquid because their θ and ϕ values should center at about 113° and 68°, respectively, from the D-12-6-1 potential.[3] None have been found in stereoplots. There is also convincing infrared evidence that any dimers in the liquid would prefer linearity.[31]

V. Conclusion

Ten years ago ab initio calculations on simple hydrogen-bonded dimers in the gas phase were rare. In the present work, an intermolecular potential function derived from a comprehensive ab initio study of the methanol dimer potential surface has been used in statistical mechanics simulations of liquid methanol. Although the optimization of the geometry for a methanol monomer with ab initio methods would have been a major undertaking a decade ago, this work illustrates that highly detailed structural information on complex liquids can now be obtained theoretically. The agreement between the Monte Carlo results and information from diffraction and infrared experiments on liquid methanol is most gratifying and auspicious for extensions even to biochemical systems. Future enhancements of computational facilities and theoretical techniques will undoubtedly be accompanied by simulations of more complex liquids and solutions with full account of intramolecular degrees of freedom, the development of more accurate and possibly transferable potential functions, and the explicit consideration of three-body and higher order interactions.

Acknowledgments. Gratitude is expressed to the National Science Foundation (CHE-7819446), Dreyfus Foundation, and Sloan Foundation for support of our research programs.

Acknowledgment is made to the donors of the Petroleum Research Fund, administered by the American Chemical Society, for support of this research. This research was also supported in part by the National Resource for Computation in Chemistry under a grant from the National Science Foundation (Grant CHE-7721305) and the Basic Energy Sciences Division of the U.S. Department of Energy (Contract No. W-7405-ENG-48). Mr. P. Cheeseman kindly provided the program to create the stereoplots.

References and Notes

(1) Quantum and Statistical Mechanical Studies of Liquids. 7. Part 6: ref 3.
(2) Camille and Henry Dreyfus Foundation Teacher-Scholar, 1978–1983; Alfred P. Sloan Foundation Fellow, 1979–1981.
(3) Jorgensen, W. L. *J. Chem. Phys.*, in press.
(4) Multhauf, R. P. "The Origins of Chemistry"; F. Watts: New York, 1966. Partington, J. R. "A History of Chemistry"; Macmillan: New York, 1964.
(5) Stinson, S. C. *Chem. Eng. News* **1979**, *57* (14), 28.
(6) Jorgensen, W. L. *J. Am. Chem. Soc.* **1979**, *101*, 2011, 2016.
(7) (a) Jorgensen, W. L. *J. Am. Chem. Soc.* **1978**, *100*, 7824. (b) *J. Chem. Phys.* **1979**, *70*, 5888.
(8) Zeiss, G. D.; Meath, W. J. *Mol. Phys.* **1977**, *33*, 1155. Dalgarno, A. *Adv. Chem. Phys.* **1967**, *12*, 143.
(9) For an important recent contribution in this area, see: Rossky, P. J.; Karplus, M. *J. Am. Chem. Soc.* **1979**, *101*, 1913.
(10) Lees, R. M.; Baker, J. G. *J. Chem. Phys.* **1968**, *48*, 5299.
(11) Weltner, W., Jr.; Pitzer, K. S. *J. Am. Chem. Soc.* **1951**, *73*, 2606. Renner, T. A.; Kucera, G. H.; Blander, M. *J. Chem. Phys.* **1977**, *66*, 177. Miller, G. A. *J. Chem. Eng. Data* **1964**, *9*, 418. Clague, A. D. H.; Govil, G; Bernstein, H. J. *Can. J. Chem.* **1969**, *47*, 625. Shuster, Ya. A.; Kozlova, V. A.; Granzhan, V. A. *Zh. Fiz. Khim.* **1978**, *52*, 799.
(12) Rahman, A.; Stillinger, F. H. *J. Chem. Phys.* **1972**, *57*, 1281.
(13) Wilhoit, R. C.; Zwolinski, B. J. *J. Phys. Chem. Ref. Data, Suppl. 1* **1973**, *2*.
(14) Wood, W. W. In "Physics of Simple Liquids", Temperley, H. N. V., Rowlinson, J. S., Rushbrooke, G. S., Eds.; Wiley-Interscience: New York, 1968.
(15) Del Bene, J. E. *J. Chem. Phys.* **1971**, *55*, 4633.
(16) Curtiss, L. A. *J. Chem. Phys.* **1977**, *67*, 1144.
(17) Hankins, D.; Moskowitz, J. W.; Stillinger, F. H. *J. Chem. Phys.* **1970**, *53*, 4544.
(18) Owicki, J. C.; Scheraga, H. *J. Am. Chem. Soc.* **1977**, *99*, 8392.
(19) Tauer, K. J.; Lipscomb, W. N. *Acta Crystallogr.* **1952**, *5*, 606.
(20) Pangali, C.; Rao, M.; Berne, B. J. *Chem. Phys. Lett.* **1978**, *55*, 413.
(21) Mezei, M.; Swaminathan, S.; Beveridge, D. L., *J. Chem. Phys.* **1979**, *71*, 3366.
(22) (a) Harvey, G. G. *J. Chem. Phys.* **1938**, *6*, 111. (b) Wertz, D. L.; Kruh, R. K. *Ibid.* **1967**, *47*, 388.
(23) The experimental studies reported $\Gamma(r) = 4\pi r^2 \rho g(r)$. From the Monte Carlo results, it is found that the locations of the peaks in the radial distribution functions are within 0.06 Å of those from $\Gamma(r)$.
(24) Narten, A. H.; Levy, H. A. *J. Chem. Phys.* **1971**, *55*, 2263. Narten, A. H. *Ibid.* **1972**, *56*, 5681.
(25) (a) Lie, G. C.; Clementi, E.; Yoshimine, M. *J. Chem. Phys.* **1976**, *64*, 2314. (b) Swaminathan, S.; Beveridge, D. L. *J. Am. Chem. Soc.* **1977**, *99*, 8392.
(26) Barker, J. A.; Fisher, R. A.; Watts, R. O. *Mol. Phys.* **1971**, *21*, 657. Halle, J. M. In "Computer Modeling of Matter", Lykos, P., Ed.; American Chemical Society: Washington, D.C., 1978; p 172.
(27) For reviews, see: Schuster, P., Zundel, G., Sandorfy, C., Eds. "The Hydrogen Bond", Vol. 1–3; North-Holland Publishing Co.: Amsterdam, 1976.
(28) Luck, W. A. P. In ref 27, p 1367.
(29) Bourdéron, C.; Pérone, J.-J.; Sandorfy, C. *J. Phys. Chem.* **1972**, *76*, 869. Bourdéron, C.; Sandorfy, C. *J. Chem. Phys.* **1973**, *59*, 2527.
(30) Olovsson, I.; Jönsson, P.-G. In ref 27, p 393.
(31) Bellamy, L. J.; Pace, R. J. *Spectrochim. Acta* **1966**, *22*, 525.

Formation of Stable Bilayer Assemblies in Dilute Aqueous Solution from Ammonium Amphiphiles with the Diphenylazomethine Segment

Toyoki Kunitake* and Yoshio Okahata

Contribution No. 513 from the Department of Organic Synthesis, Faculty of Engineering, Kyushu University, Fukuoka, 812, Japan.
Received March 5, 1979

Abstract: Quaternary ammonium amphiphiles of the following structures were synthesized: C_n-BB-N^+3C_1 and C_n-BB-C_m-N^+3C_1, where C_n and C_m are hydrocarbon chains of n = 0, 4, 7, 12 and m = 4, 10, and BB and N^+3C_1 denote 4,4′-diphenylazomethine moiety and trimethylammonium group, respectively. These amphiphiles gave clear or slightly turbid solutions when dispersed in water by the sonication or injection method. The aqueous solutions contained extraordinarily large aggregates: 10^6–10^7 daltons except for BB-N^+3C_1 and C_4-BB-N^+3C_1, as estimated by the light scattering method. The critical micelle concentration was 10^{-4}–10^{-5} M when the hydrocarbon tail (C_n portion) was present. Electron microscopy indicated that these aggregates (n = 7 and 10) possessed lamellar or vesicle structures which were composed of the bilayer assembly (layer thickness 40–60 Å). The bilayer structure could not be detected for amphiphiles of n = 0 and 4. The C_m portion did not appear to affect the aggregate structure. NMR spectroscopy and differential scanning calorimetry suggested the liquid crystalline property of these aqueous aggregates. In conclusion, the stable bilayer assembly similar to that of biomembranes was prepared in dilute aqueous solution from single-chain ammonium amphiphiles which possessed a rigid segment.

The major components of the lipid bilayer of biomembranes are phospholipids which possess two long alkyl chains. The reason why these biolipids produce at low concentrations the bilayer structure instead of globular micelles has been frequently discussed.[1,2] Among various structural features the existence of the two alkyl chains was shown to be essential for the bilayer formation by recent developments in these laboratories that stable bilayer assemblies were readily formed from a variety of synthetic dialkyl amphiphiles of C_{10}–C_{18}. The hydrophilic group of these amphiphiles may be cationic (ammonium and sulfonium),[3-5] anionic (sulfonate, phosphate, and carboxylate),[6] nonionic (polyoxyethylene),[7] or zwitterionic.[7] Similar studies were reported by other workers.[8-10]

On the other hand, we suspected that the liquid-crystalline nature of bilayers (both natural and synthetic) is the cause and not the result of the bilayer formation. Then it should be possible to find bilayer-forming amphiphiles whose structures are quite different from those of dialkyl amphiphiles. Diphenylazomethine derivatives belong to a major class of liquid-crystalline materials.[11] Therefore, we prepared a series of ammonium amphiphiles which possess the diphenylazomethine moiety and studied their aggregation behavior in *dilute*

0002-7863/80/1502-0549$01.00/0